Characteristics of Zinc-Doped Hydroxyapatite Prepared Using Biogenic and Synthetic Calcium Precursor

C. M. Mardziah, N. R. N. Masdek, N. M. Mubarak, and S. Ramesh

Abstract Hydroxyapatite (HA) bioceramic has been used for clinical applications due mainly to its chemical similarity with human bones. However a major drawback with HA synthesized by using commercial sources is the absences of ions such as zinc which is normally found in natural bone. In this work, comparison between the characteristics of zinc HA powders synthesized using different source of calcium precursor (commercial and waste eggshells) were studied. Both powders were prepared through wet chemical precipitation method using the same phosphorous and zinc reagents, under the exact experimental conditions. The physicochemical properties of these powders before and after undergoing calcination at 700 °C were examined. This study demonstrated how the characteristics of the synthesized powders slightly differ in terms of their thermal stability and molecular structure due to the use of different calcium source. The study found that the addition of zinc ion in powders prepared using commercial calcium source led to higher formation of secondary phase, β-TCP than the powder prepared using eggshell calcium.

Keywords Calcium precursor · Chemical precipitation · Waste eggshell · Zinc hydroxyapatite

1 Introduction

Synthetic hydroxyapatite [HA, $Ca_{10}(OH)_2(PO_4)_6$] has been widely used as implant material in biomedical field since many decades ago due to its chemical properties

C. M. Mardziah (✉) · N. R. N. Masdek
School of Mechanical Engineering, College of Engineering, Universiti Teknologi MARA, Selangor Darul Ehsan, 40450 Shah Alam, Malaysia
e-mail: mardziah31@uitm.edu.my

N. M. Mubarak · S. Ramesh
Faculty of Engineering, Universiti Teknologi Brunei, Tungku Highway, Gadong 1410, Brunei Darussalam

S. Ramesh
Center of Advanced Manufacturing and Material Processing, Department of Mechanical Engineering, Faculty of Engineering, University of Malaya, 50603 Kuala Lumpur, Malaysia

Md. A. Maleque et al. (eds.), *Proceeding of 5th International Conference on Advances in Manufacturing and Materials Engineering*, Lecture Notes in Mechanical Engineering,
https://doi.org/10.1007/978-981-19-9509-5_24

that has close resemblance to the natural bone. One of the important features of HA is its capacity for ionic substitution. This means that the locations for hydroxyl, phosphate and calcium ions may be occupied by ions of a similar size and charge without disrupting the HA structure [1]. There has been a substantial effort made by numerous investigators to improve the overall properties of synthetic HA. One of the strategies is to introduce metallic ions into HA such as magnesium [2, 3], manganese [4], zinc [5], bismuth [6], and strontium [7].

Traces of metal ions can influence the lattice parameters, the crystallinity, the dissolution kinetics, increase chemical affinity and other physical properties of apatite [8]. They are also believed to have significant role towards improving cell-material interactions of HA and strengthening its mechanical properties, which is beneficial in the bone remodeling process. This strategy of incorporating metal ions and other minute dopants or additives, particularly that of transition metal oxides, during processing have also been shown to be successful and economical means of enhancing the properties of other materials during powder consolidation, promoting microstructure refinement during joining or welding, and in the tailoring of suitable microstructure-properties for a host of applications [9–17].

Amongst the transition metal oxides, zinc is recognized as an essential trace element in the human body due to its vital role in the development of skeletal system and normal biological growth. In addition, zinc inhibits osteogenic differentiation, stimulates osteoblasts activity and regulate cell biological response [18]. Zinc deficiency not only is associated with serious malnutrition problem but was also reportedly related to the impairment of maximal bone mass development [19], which increases the risk of osteoporotic bone. Zinc ions with approximately 0.012–0.025 wt% are found in all tissues of the human body, and most of them is stored in the skeleton [19]. It plays a major role in homeostasis, immune response, metabolic function, wound healing, oxidative stress and few other physiological systems in mammals.

Although several works on zinc substituted HA have been previously reported, they were mainly synthesized using commercial calcium sources. In this present study, zinc-doped HA (ZnHA-Es) bioceramic was prepared using waste chicken eggshells as its calcium precursor with 3 mol% of zinc ion incorporation. The samples were calcined at 700 °C and then compared to ZnHA, which was prepared using commercial calcium precursor under the same experimental conditions.

2 Materials and Method

For the preparation of ZnHA, commercial CaO powders (Systerm Chemicals) and ammonium di-hydrogen phosphate ($NH_4H_2PO_4$) (R&M Chemicals) were used as a calcium and phosphorus precursor, respectively whilst the zinc ion source was zinc nitrate ($Zn(NO_3)_2$) from Sigma-Aldrich. On the other hand, for ZnHA-Es, the calcium eggshell (CaO-Es) was used in place of commercial CaO but for the other two precursors (phosphorous and zinc), the chemicals remained the same. It should

be noted that, the amount of zinc dopant incorporated in both type of samples was 3 mol%. In addition, ammonia solution (NH_4OH) from R&M Chemicals was used to increase the solution's pH.

In this work the eggshells were cleaned in hot water, crushed, and heat-treated at 700 °C for 1 h. The calcined powder was sieved to obtained the CaO-Es. Before the final mixing, each precursor was dissolved separately using distilled water on a hotplate magnetic stirrer until they became homogenous. $NH_4H_2PO_4$ and $Zn(NO_3)_2$ were slowly added into $Ca(OH)_2$ solution and after that the NH_4OH was added little by little to increase the solution's pH to 10.5. The solution mixture was constantly stirred for 3 h while the reaction temperature was maintained at 90 °C. The precipitates were aged for 24 h, filtered and washed with deionized water to rinse away any contaminants that were still clinging on the precipitates. After that, they were dried overnight in an oven at 100 °C to remove excess water. All synthesized powders were subjected to calcination at 700 °C with a heating rate of 5 °C/min and a 2-h holding time. Calcination at this temperature was carried out to eliminate volatile substances present in the samples as well as to compare the powders characteristics between ZnHA-Es and ZnHA.

Phase identification and quantification in this study were conducted using X-Ray diffractometer (Rigaku Ultima IV) with a scan speed of 5°/min between 20 and 60°. The diffraction peaks were indexed according to International Centre for Diffraction Data (ICDD) PDF card number 01-079-5683, 01-086-1585, 01-080-2801, 01-077-9574 and 01-076-0571 for HA, β-TCP, $CaCO_3$, CaO and $Ca(OH)_2$, respectively.

For molecular structure identification, the IR spectra of the samples were recorded using a Fourier transform infrared (FTIR) spectrometer (Perkin Elmer) in a frequency range of 500–4000 cm^{-1}.

The microstructures of calcined samples were examined using field emission electron microscopy (FESEM) (FEI Quata FEG450), which was also equipped with a built-in Energy Dispersive X-Ray (EDX) system to perform elemental analysis on the targeted samples. For clearer images, these samples were first coated with platinum (Pt) using sputter coater (Polaron, SC7620) prior observation under FESEM.

3 Results and Discussion

The XRD phase analysis of the commercial CaO and CaO-Es are shown in Fig. 1a. Both powders consist of three CaO signature peaks at 2θ degree of 32°, 37° and 54°. No other impurities were detected in both type of powders. It is crucial that the CaO-Es powders have excellent purity so that only an accurate amount of CaO-Es will be used as a reagent during the synthesis process.

The FTIR spectrum of CaO-Es shown in Fig. 1b, has close similarity with the spectrum of commercial CaO powders. Both indicate characteristic bands inherent to CaO structure, which contain carbonate and hydroxyl frequency bands. The broad carbonate bands at 2329, 1430 and 1056 cm^{-1} are associated with stretching mode

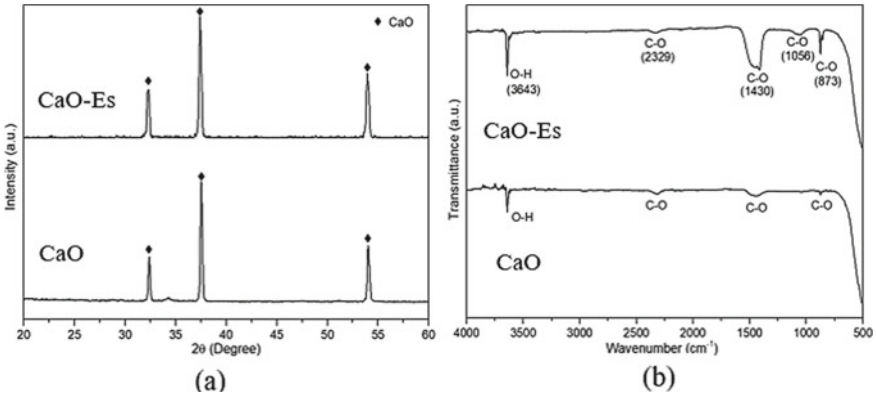

Fig. 1 Comparison between commercial CaO and eggshell derived CaO-Es in **a** XRD patterns and **b** FTIR spectrum

with respect to adsorbed CO_2 on the surface of CaO, while a sharp peak at 3643 cm^{-1} corresponds to hydroxyl band. Another sharp frequency band which also belongs to C–O group was observed at 873 cm^{-1} [20].

XRD patterns in Fig. 2 indicate that after calcination at 700 °C, both samples contain a mixture of HA and β-TCP phases. The main HA peaks were indexed at 32°, 32.3° and 33° in accordance to the ICDD standard for HA phase. Formation of β-TCP phase was confirmed by the appearance of a low intensity peak at approximately 31°, which is common when there is a presence of impurities like zinc ion in HA. Peak shifting was not observed in the present work. It is also evident that the ZnHA-Es was as crystalline as the ZnHA powders. However, the formation of secondary phase was apparently much higher in ZnHA compared to ZnHA-Es as indicated by the intensity of the β-TCP peak. Based on this calcination study, it can be deduced that HA phase for powders produced using commercial calcium most likely tend to decompose to β-TCP phase more rapidly compared to samples prepared using natural calcium.

The microstructure evolution of the ZnHA-Es and ZnHA calcined powders is presented in Fig. 3.

The SEM micrographs revealed that the powders consist of fine spherical-like particles of varying sizes. It was also observed that the microstructure of ZnHA-Es exhibited somewhat larger particles (D_{ave} ~ 100 nm) compared to the ZnHA (D_{ave} ~ 40–50 nm) samples. On the other hand, Ca/P ratio approximation based on EDX analysis shows that ZnHA-Es has Ca/P ratio 1.65 while for ZnHA, the ratio was 1.56.

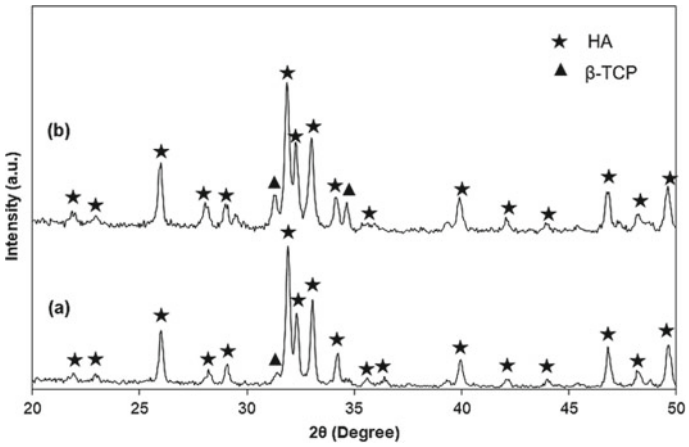

Fig. 2 XRD patterns of **a** ZnHA-Es and **b** ZnHA samples after calcination at 700 °C

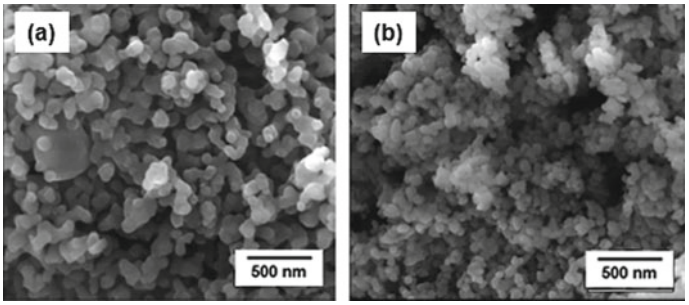

Fig. 3 FESEM micrographs (mag. × 20 k) of **a** ZnHA-Es and **b** ZnHA powders

4 Conclusions

In this study, nanostructured ZnHA-Es and ZnHA powders were successfully prepared via precipitation method using calcium precursor derived from waste eggshells and commercial calcium, respectively. XRD results showed that the powders had become crystalline after calcination at 700 °C, with an apparent formation of biphasic mixture, HA and β-TCP in both samples. Agglomeration of powder aggregates (~ 40 to 100 nm in size) was clearly noticed from FESEM images for both samples which is typical for nano-powders. Ca/P ratio of ZnHA-Es was found to be close to stoichiometric HA with 1.65 but on the contrary, the Ca/P ratio of ZnHA was much lower at 1.57, which indicates that it is calcium-deficient. The findings of this work suggested that ZnHA-Es and ZnHA has slightly different physicochemical properties, but both can still possibly be potential candidates as bio-implant material.

Acknowledgements This work was funded by Ministry of Higher Education Malaysia (MOHE) under Grant No. FRGS/1/2018/TK05/UITM/02/18 and FP020-2018A. We would also like to acknowledge Universiti Teknologi MARA (UiTM) and University of Malaya (UM) for providing laboratory facilities and technical supports.

References

1. Kolmas J, Groszyk E, Kwiatkowska-Rózycka D (2014) Substituted hydroxyapatites with antibacterial properties. Biomed Res Int 2014(2):178123
2. Nabiyouni M, Ren Y, Bhaduri SB (2015) Magnesium substitution in the structure of orthopedic nanoparticles: a comparison between amorphous magnesium phosphates, calcium magnesium phosphates and hydroxyapatites. Mater Sci Eng C 52:11–17
3. Tan CY, Yaghoubi A, Ramesh S, Adzila S, Purbolaksono J, Hassan MA, Kutty MG (2013) Sintering and mechanical properties of MgO-doped nanocrystalline hydroxyapatite. Ceram Int 39:8979–8983
4. Pandya HM, Anitha P (2015) Influence of manganese on the synthesis of nano hydroxyapatite by wet chemical method for in vitro applications. Am J Phytomedicine Clin Ther 2(4):394–402
5. Tank KP, Chudasama KS, Thaker VS, Joshi MJ (2014) Pure and zinc doped nano-hydroxyapatite: synthesis, characterization, antimicrobial and hemolytic studies. J Cryst Growth 401:474–479
6. Ramesh S, Tan CY, Yeo WH, Tolouei R, Amiriyan M, Sopyan I, Teng WD (2011) Effects of bismuth oxide on the sinterability of hydroxyapatite. Ceram Int 37:599–606
7. Sanyal V, Raja CR (2016) Synthesis, characterization and in-vitro studies of strontium-zinc co-substituted fluorohydroxyapatite for biomedical applications. J Non Cryst Solids 81–87
8. Forero-Sossa PA, Olvera-Alvarez IU, Salazar-Martinez JD, Espinosa-Arbelaez DG, Segura-Giraldo B, Giraldo-Betancur AL (2021) Biogenic hydroxyapatite powders: effects of source and processing methodologies on physicochemical properties and bioactive response. Mater Charact 173:1–14
9. Ramesh S, Sara Lee KY, Tan CY (2018) A review on the hydrothermal ageing behaviour of Y-TZP ceramics. Ceram Int 44:20620–20634
10. Duraisamy N, Numan A, Ramesh K, Choi K-H, Ramesh S, Ramesh S (2015) Investigation on structural and electrochemical properties of binder free nanostructured nickel oxide thin film. Mater Lett 161:694–697
11. Bowen C, Ramesh S, Gill C, Lawson S (1998) Impedance spectroscopy of CuO-doped Y-TZP ceramics. J Mater Sci 33:5103–5110
12. Manladan SM, Yusof F, Ramesh S, Zhang Y, Luo Z, Ling Z (2017) Microstructure and mechanical properties of resistance spot welded in welding-brazing mode and resistance element welded magnesium alloy/austenitic stainless steel joints. J Mater Process Technol 250:45–54
13. Ramesh S, Zulkifli N, Tan CY, Wong YH, Tarlochan F, Ramesh S, Teng WD, Sopyan I, Bang LT, Sarhan AAD (2018) Comparison between microwave and conventional sintering on the properties and microstructural evolution of tetragonal zirconia. Ceram Int 44:8922–8927
14. Sampath Udeni Gunathilake TM, Ching YC, Chuah CH, Illias HA, Ching KY, Singh R, Nai-Shang L (2018) Influence of a nonionic surfactant on curcumin delivery of nanocellulose reinforced chitosan hydrogel. Int J Biol Macromolecules 118:1055–1064
15. Francis KA, Liew C-W, Ramesh S, Ramesh K, Ramesh S (2016) Ionic liquid enhanced magnesium-based polymer electrolytes for electrical double-layer capacitors. Ionics 22:919–925
16. Ramesh S, Amiriyan M, Meenaloshini S, Tolouei R, Hamdi M, Purboloksono J, Teng WD (2011) Densification behaviour and properties of manganese oxide doped Y-TZP ceramics. Ceram Int 37:3583–3590

17. Azim Jais A, Muhammed Ali SA, Anwar M, Rao SM, Muchtar A, Wan Isahak WNR, Tan CY, Singh R, Brandon NP (2017) Enhanced ionic conductivity of scandia-ceria-stabilized-zirconia (10Sc1CeSZ) electrolyte synthesized by the microwave-assisted glycine nitrate process. Ceram Int 43:8119–8125
18. Cama G, Nkhwa S, Gharibi B, Lagazzo A, Cabella R, Carbone C, Dubruel P, Haugen H, Di Silvio L, Deb S (2017) The role of new zinc incorporated monetite cements on osteogenic differentiation of human mesenchymal stem cells. Mater Sci Eng C 78:485–494
19. Luo X, Barbieri D, Davison N, De Bruijn JD, Yuan H (2014) Zinc in calcium phosphate mediates bone induction: in vitro and in vivo model. Acta Biomater 10:477
20. Kamalanathan P, Ramesh S, Bang LT, Niakan A, Tan CY, Purbolaksono J, Hari Chandran Teng WD (2014) Synthesis and sintering of hydroxyapatite derived from eggshells as a calcium precursor. Ceram Int 40:16349–16359